Environ. Sci. Technol. **2010,** *44,* 7425–7430

Global Concentrations of Gaseous Elemental Mercury and Reactive Gaseous Mercury in the Marine Boundary Layer

ANNE L. SOERENSEN,*,† HENRIK SKOV,† DANIEL J. JACOB,‡ BRITT T. SOERENSEN,†,§ AND MATTHEW S. JOHNSON§

National Environmental Research Institute, Aarhus University, Frederiksborgvej 399, DK-4000 Roskilde, Denmark, School of Engineering and Applied Sciences and Department of Earth and Planetary Sciences, Harvard University, Cambridge Massachusetts 02138, and Copenhagen Center for Atmospheric Research, Department of Chemistry, University of Copenhagen, Universitetsparken 5, DK-2100 Copenhagen, Denmark

Received December 18, 2009. Revised manuscript received August 20, 2010. Accepted August 24, 2010.

Gaseous elemental mercury (GEM) and reactive gaseous mercury (RGM) were measured during an eight month circumnavigation to obtain knowledge of their worldwide distributions in the marine boundary layer (MBL). Background GEM concentrations were found to be 1.32 ± 0.2 ng/m^3 (summer) and 2.62 ± 0.4 ng/m^3 (spring) in the northern hemisphere and 1.27 ± 0.2 ng/m^3 (spring and summer) in the southern hemisphere. Radiation and relative humidity are shown to control diurnal cycles of RGM. During the cruise the ship passed areas of clean MBL air, air influenced by biomass burning (South Atlantic) and air with high concentrations of GEM and RGM of unknown origin (Antarctic). High GEM concentrations above the Atlantic indicate that emission from the ocean can be an important GEM source. Our data combined with data from earlier cruises provides adequate information to establish a seasonal cycle for the Atlantic. Results show a cycle similar to that found at Mace Head, Ireland but with larger amplitude. We have improved the basic knowledge of mean GEM and RGM concentrations in the MBL worldwide and shown how natural sources and reemissions can affect GEM concentrations in the MBL.

Introduction

Mercury biomagnifies in the food web, and the consumption of aquatic animals in particular is a human health issue (*1*). Deposition from the atmosphere is the major source of mercury to the ocean (*2*) and there is a fast equilibrium of mercury between the marine boundary layer (MBL) and the surface ocean through air-sea exchange (*3*). Despite this there is a lack of knowledge of the dynamics of mercury in the MBL (*2*). This knowledge is important if we want to understand anthropogenic impact on the ocean and constrain modeling of air−sea interactions (*4*).

Here we present results from measurements of gaseous elemental mercury (GEM) and reactive gaseous mercury (RGM) from an eight month marine circumnavigation of the globe. The results provide new insight into concentrations and behavior of GEM and RGM in the MBL and provide information on air−sea interactions.

Observations of mercury in the MBL are sparse compared to those in the terrestrial boundary layer. In most cases only GEM (or total gaseous mercury) has been measured (e.g., refs *5*−*9*), whereas supplementary measurements of other mercury species have been obtained on only a few occasions in the major ocean basins (*10*−*14*).

A gradient of GEM concentrations in the MBL between the NH (northern hemisphere) and SH (southern hemisphere) has been established (*6, 8*) with a trend similar to the one found at terrestrial sites (*2*). In the NH there is considerable variation in concentrations measured on cruises while concentrations in the SH seem to be more uniform (*8*). Average results from cruise campaigns range from 1.5 ng/m^3 (*10*) to 2.3 ng/m^3 (*6*) in the northern Atlantic Ocean (>10°N) and up to 2.5 ng/m^3 in the northern Pacific Ocean (*11*). In the NH MBL concentrations are therefore often well above terrestrial background concentrations (1.5−1.7 ng/m^3 (*2*)).

Sources are estimated to contribute 2700−7100 ton Hg/a from natural emissions and reemissions and 1200−2900 ton Hg/a from direct anthropogenic emissions (*15*). Emissions from the ocean are not well constrained and estimates of net evasion range from 800 ton/a (*16*) to 2800 ton/a (*3*). Both anthropogenic and oceanic sources could be important factors in controlling high MBL mercury concentrations.

While the lifetime of GEM is estimated to be from months to 1.5 years in the troposphere (*17*) it could be as low as weeks for the MBL (*18*) and hours in the Polar spring (*19*). For the troposphere the lifetime of GEM is long enough to support transport over synoptic scales and thus it is ubiquitous.

RGM consists of one or more unidentified Hg^{II} compounds, which may differ in concentration in time and space. RGM is adsorbed much faster on surfaces than GEM (*2*) and has a shorter lifetime in the atmosphere. Anthropogenic RGM therefore mainly affects areas close to the source, while the oxidation of GEM continuously resupplies RGM to the MBL, where RGM concentrations are kept low by uptake on sea spray or dry deposition (*11, 20*). Mean RGM concentrations for recent cruise campaigns are between 2.4−10 pg/m^3 (*10*−*12, 14*). In agreement with this general understanding of the RGM dynamics, diurnal cycles with peaks at midday/afternoon have been found at sites in the MBL (*11, 12, 20*). This indicates that the oxidation is photochemically mediated, and its removal is fast enough to decrease concentrations during the night (*21*), when RGM production does not take place. A correlation with wind speed and relative humidity (RH) has been reported for RGM (*11, 20*) due to increased dry deposition and uptake on sea spray under conditions of high wind speed, and increased uptake on water droplets with increased RH. Although it is unclear which oxidant dominates on a global scale, analysis of atmospheric depletion events in the Arctic have shown that Br atoms are the dominant oxidant in polar regions (*22*) resulting in a lifetime of GEM of hours (*19, 23*). Br atoms could also be the primary oxidant in the MBL (*21*) where it is released from sea salt aerosols (*24*).

The main object of this work is to investigate the spatial distribution of GEM and RGM in the MBL around the world. The focus is on the mechanisms driving concentrations, as the effects of regional sources and photochemistry within

* Corresponding author phone: +45 4630 1154; e-mail: anls@dmu.dk.
† Aarhus University.
‡ Harvard University.
§ University of Copenhagen.

10.1021/es903839n
Published on Web 09/07/2010

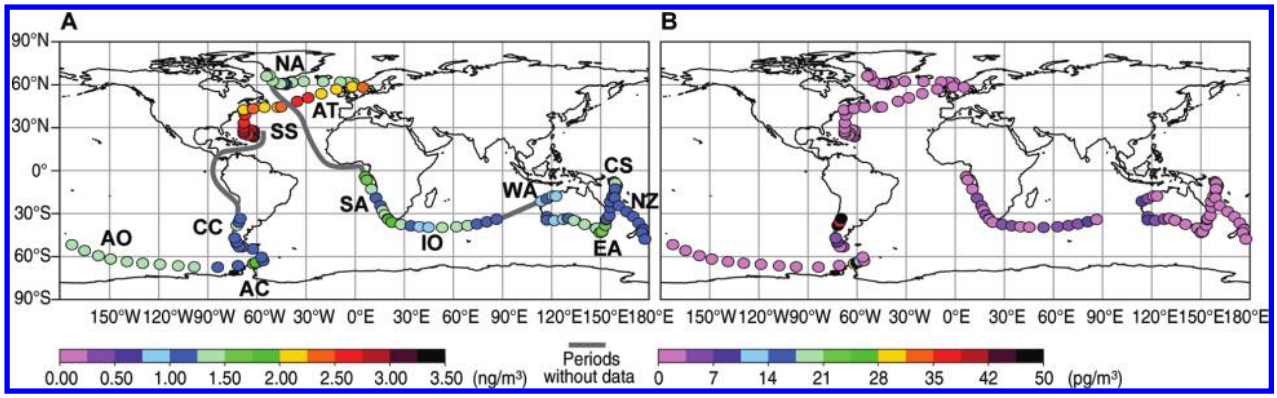

FIGURE 1. The navigation route of the *Galathea 3* expedition. Shown are daily mean concentrations of (A) GEM and (B) RGM. The gray line indicates the route during periods without measurements and the names are the abbreviations of the 12 cruise legs. A list of abbreviations is found in Table 1. The cruise covered 39 000 nautical miles.

the MBL changes. The results will help constrain models and further improve understanding of the processes that control the dynamics of mercury in the troposphere.

Materials and Methods

Measurements of GEM and RGM were carried out continuously through an eight month circumnavigation with *Galathea 3*. The cruise started August 10th 2006 and ended on April 25th 2007 in Copenhagen, Denmark. Details of the cruise legs are shown in Figure 1 and Table 1.

GEM and RGM were measured using a TEKRAN 2537A mercury vapor analyzer equipped with a TEKRAN 1130 automated denuder unit and pump module. The TEKRAN system was programmed so that GEM was measured at 5 min intervals for a period of 80 min. During this period RGM was sampled on an annular quartz denuder. This was followed by a 40 min period in which RGM sampled on the denuder was determined by thermal desorption and analyzed with the TEKRAN 2537A.

The detection limit of GEM is 0.1 ng/m^3 (*19*). The method detection limit for RGM was calculated as 3 × std. dev. on blank values obtained during the analysis of the annular quartz denuder and was always better than 2 pg/m^3. The stability of the instrument was checked by parallel measurements with two TEKRAN 2537A instruments. The response of the detector was checked every 25 h by adding clean air and air with a known amount of Hg^0 from an internally thermostatted permeation tube. Before and after the cruise the permeation rate was determined using manual injections of known quantities of mercury, and it was found to be constant. The reproducibility of GEM measurements is 20% at a 95% confidence interval above 0.5 ng/m^3, and of RGM measurements, 28% (Supporting Information SI T2). Along the coast of Africa the addition from the permeation source was missing for 22 days. Fortunately the detector signal only drifted a few percent during this time and we applied a linear interpolation spanning the period. The resulting uncertainty is minimal.

Supplementary measurements of NO_x, soot and standard meteorological variables were available for parts of the cruise (SI T3, Ta1). NO_x was used to indicate local contamination from the ship. In agreement with the results of Sommar et al. (*9*) smoke from the ship was not found to contaminate mercury measurements.

Results and Discussion

Average Global and Hemispheric Concentrations. GEM and RGM data are presented in Figure 1, Table 1 and SI S1. Our GEM data supplement previously published cruise data during some parts of the cruise but also present data from areas that have so far not been investigated, such as parts of the South Pacific Ocean (Coral Sea, Tasman Sea, coast of Chile) and part of the Southern Ocean. Our data overlap with existing measurements (SI Ta2) above the eastern Atlantic (*5, 6, 8*), the North Atlantic and coast of Greenland (*9*), above the Sargasso Sea (*12, 13*), the Indian Ocean (*25*), and during the Antarctic to South American leg (*14*). For RGM overlap only occurs in the Sargasso Sea (*12, 13*) and during the Antarctic to South America leg (*14*).

GEM measurements are significantly different between spring (2.62 ± 0.4 ng/m^3, $n = 241$) and late summer (1.32 ± 0.2 ng/m^3, $n = 190$) in the NH ($P < 0.001$). In the SH the average concentration was 1.27 ± 0.2 ng/m^3 ($n = 848$), which is significantly lower than both averages from the NH ($P < 0.05$). Thus our measurements confirm the hemispheric gradient observed by others (*6−8, 26*).

Some of our observations in the NH falls outside of the range of earlier observed MBL concentrations in the NH. This will be discussed thoroughly later.

Earlier studies of GEM in the SH Atlantic (*6, 8, 25*) show uniform concentrations despite changes in latitude. Our data confirm that the uniformity of concentration (>10°S) includes all SH ocean basins and is within the values expected based on background concentrations from terrestrial sites (1.1−1.3 ng/m^3 (*2*)).

The global mean of RGM in the free MBL was 3.1 ± 11 pg/m^3 ($n = 1174$). This is in agreement with published measurements of RGM in the MBL, except for one study with high values (50−700 pg/m^3) (*13*). Mean concentrations of 2.5−10 pg/m^3 have previously been found between Antarctica and South America (*14*), and in the North Atlantic (*10*) and the Atlantic (*12*) and Pacific Oceans (*11*). Our measurements complement earlier measurements to give a picture of uniformly low RGM in the MBL worldwide.

Diurnal Cycles of Gaseous Mercury Species. Data were broken into 12 legs based on ocean basin and origin of air mass (Table 1). Dividing RGM in these legs into daytime (6−18) and nighttime (18−6, local time) values revealed a significant ($P < 0.1$) diurnal variation with midday peaks in 5 of the 12 legs (Figure 2, Table 1). Legs with a diurnal variation in RGM as well as the AT (Atlantic Ocean) leg showed a positive correlation with radiation and negative correlation with RH (Table 1). This was apparent for each leg, when splitting days into six four-hour intervals, which were then averaged for each leg, giving a mean diurnal cycle of six intervals as seen in Figure 2. Diurnal cycles in the MBL have earlier been found in the Pacific Ocean (*11*) and the Sargasso Sea (*12*) and indicate photochemical RGM formation.

A common feature for the NA (North Atlantic), AO (Antarctic Ocean) and AT legs, which all lack diurnal variation, is a mean RH above 90% and low insolation. Mean incoming insolation at midday (11−13, local time) during the AO was

TABLE 1. Global, Hemispheric and Sectional Data from the *Galathea 3* Cruise

leg	Ab[a]	dates	lat[b] (deg)	origin[c]	GEM (ng/m^3) mean(±std)	RGM (pg/m^3) mean(±std)	no obs GEM/RGM	RGM *t* test day vs night	RGM-Rad[d] PCC	RGM-RH[d] PCC
Global		16th August to 24th April	−65: 67		1.53(±0.58)	3.1(±11)	1279/1174			
NH summer		16th August to 1st September	58: 67		1.32(±0.16)	0.4(±3)	190/172			
NH spring		30th March to 24th April	23: 59		2.61(±0.36)	0.8(±2)	241/218			
SH		8th October to 8th February	−65: −3		1.27(±0.25)	4.3(±14)	848/784			
North Atlantic	NA	16th August to 1st September	58: 67	ocean	1.32(±0.16)	0.4(±3)	190/172			0.31
Atlantic O.	AT	15th April to 24th April	43: 59	ocean	2.26(±0.26)	0.1(±1)	100/92		0.89[f]	−0.83[f]
Sargasso Sea	SS	30th March to 11th April	23: 45	mixed	2.86(±0.17)	1.2(±2)	141/126		−0.49	0.31
South Africa	SA	8th October to 21st October	−39: −3	mixed	1.36(±0.24)	3.4(±4)	113/101		−0.60	0.43
Indian Ocean	IO	22nd October to 29th October	−39: −33	ocean	1.11(±0.19)	4.6(±5)	88/79	[e]	0.83[f]	−0.66[(0.16)]
West Australia	WA	3rd November to 6th November	−22: −17	ocean	1.03(±0.16)	5.0(±6)	32/26	[g]	0.77[e]	−0.94[g]
East Australia	EA	23rd November to 15th December	−44: −26	mixed	1.33(±0.24)	1.9(±3)	185/175	[e]	0.94[g]	−0.77[e]
Coral Sea	CS	16th December to 3rd January	−27: −7	mixed	1.21(±0.18)	0.3(±1)	130/124	[g]	0.71[0.11]	−0.89[f]
New Zealand	NZ	3rd January to 14th January	−56: −26	mixed	1.19(±0.17)	0.1(±0)	108/104	[g]	0.89[f]	−0.83[f]
Antarctic O.	AO	14th January to 24th January	−65: −55	ocean	1.30(±0.16)	0.0(±0)	105/92		0.09	−0.09
Antarctic Coast	AC	25th January to 28th January	−65: −63	mixed	1.55(±0.38)	43.0(±39)	49/47		−0.2	−0.03
Coast of Chile	CC	31st January to 8th February	−58: −33	mixed	1.11(±0.11)	28.6(±30)	37/36		−0.49	0.54

[a] Abbreviations used in the text. [b] The latitude that the given leg includes. [c] Ocean = no influence from terrestrial sources, Mixed = influence from terrestrial sources during the entire or smaller but significant portions of the leg. [d] PCC (r) = Pearson's correlation coefficient (with significance level given in footnotes e−h. [e] $P < 0.1$. [f] $P < 0.05$. [g] $P < 0.01$.)

low with 235 W/m^2 (we do not have observations of radiation from the NA leg) (SI Ta1). The AT leg did not show a significant difference between RGM concentrations during daytime and nighttime but did show significant correlation with radiation and anticorrelation with RH ($P > 0.01$). A closer look at the leg showed that RGM cycles were present when insolation was >500 W/m^2 and RH <90% but not when it was below <350 W/m^2. The lowest mean for a leg with a diurnal RGM cycle occurred on the NZ (New Zealand) leg with mean incoming solar radiation of 493 W/m^2. A lack of diurnal variation has previously been observed in the Arctic (*9, 10*) and was suggested to be a consequence of high RH, fog, and insolation below 200 W/m^2 (*10*). Our data support the importance of these variables.

We did not observe any diurnal variability during the SA (South Africa), CC (Coast of Chile), SS (Sargasso Sea), and AC (Arctic coast) legs (Figure 2). For the SA and CC legs ancillary data and back trajectories showed the influence of biomass burning and anthropogenic emissions explaining the cycle's absence. For the SS leg we do no have an explanation for the lack of diurnal variation, which has previously been observed in the Sargasso Sea (*12*). The AC (Antarctic coast) leg is a special case and will be discussed separately later.

Radiation seems to control the diurnal cycle of RGM in the MBL by controlling the GEM oxidation potential and possibly by influencing RH, shifting the equilibrium of RGM between air and the aqueous phase. Under low-radiation conditions when RH > 90% the diurnal cycle disappears due to damped photochemistry combined with an increased potential for sorption of RGM in to the aqueous phase of aerosols.

A nightly decline in RGM with increasing wind speed for individual legs as proposed by Holmes et al. (*21*) was not observed, although some legs (NZ, EA (East Australia), CS (Coral Sea), AC) show an overall anticorrelation with wind speed.

Earlier cruises have reported both the absence and the presence of diurnal GEM cycles even within the same campaign (*9, 11*). In contrast we did not observe diurnal cycles of GEM.

GEM above the Atlantic Ocean (NH). For the Atlantic Ocean measurements are available from both August 2006 and April 2007. Measurements from August (NA leg) were low (1.32 ± 0.2 ng/m^3, $n = 190$) compared to previous August cruises (Figure 3) (*5, 9, 12*). The air that arrived at the ship came from a non ice-covered Arctic Ocean (determined by back trajectories (*27*)). During June 2004 and July 2007 cruises in the same area found GEM concentrations around 1.5 ng/m^3 (*10*) and 1.7 ng/m^3 (*9*), respectively. Thus our observations are at the low end of earlier summertime observations in the area.

The SS leg during April 2007 had the highest GEM concentrations of the campaign. The mean concentration during the 13 days spent 1000−1500 km from the coast was 2.86 ± 0.17 ng/m^3 ($n = 141$). RGM did not increase above background concentrations. Back trajectory analyses show that air came from a broad range of North American locations, with 1−3 days in the MBL before reaching the ship. The location seems too remote and the source area too large for anthropogenic plumes to be the sole explanation. During a spring cruise in the Pacific Ocean a mean concentration of 2.5 ng/m^3 was found (*11*) indicating that spring could be a period of high MBL concentrations. A combination of high evasion from the ocean during spring (*4*) and anthropogenic influence might explain the high concentrations observed, but we do not fully understand the observations.

During the AT leg in April 2007 GEM concentrations (2.26 ± 0.26 ng/m^3, $n = 100$) were lower than during the SS leg, but still elevated compared to the rest of the cruise. No other cruises that we know of have taken place in the Atlantic Ocean

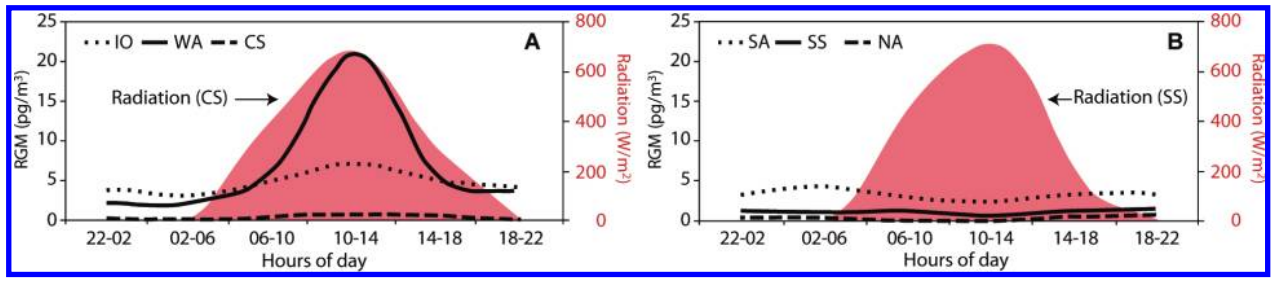

FIGURE 2. Examples of diurnal cycles of RGM and radiation during (A) selected legs that show diurnal variation and, (B) selected legs that do not show diurnal variation due to low radiation and RH > 90%, or anthropogenic/biomass burning influence. A list of abbreviations is found in Table 1.

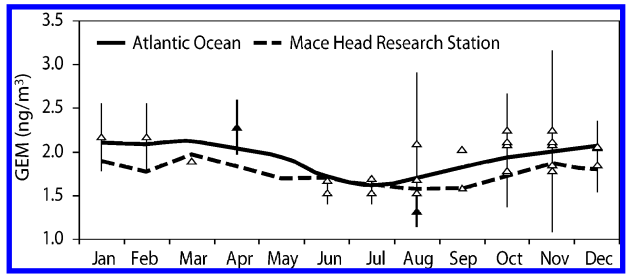

FIGURE 3. GEM seasonal cycle in the MBL (black line) (based on the data from this (▲) and previous studies (*5*–*7, 10, 12, 13*) (Δ)) and at Mace Head (1995–2001) (hatched line) (*28*). Standard deviations for single studies are shown where the information is available. Further explanation of the method of calculation of the GEM cycle for the Atlantic MBL is found in SI T2.

during this season. After leaving the Boston harbor winds were northerly, temperature low and a single atmospheric depletion event with GEM below the detection limit was observed. The highest GEM concentrations were seen in the middle of the Atlantic basin when back trajectories, wind direction and temperature indicated southerly origin of the air from the Atlantic MBL between 30–50° N for at least 5 days. Thus the high concentrations must have an oceanic source. Back trajectories for the three legs are shown in SI S2.

The Research station Mace Head at the western tip of Ireland receives air primarily from the Atlantic Ocean. Evasion from the Atlantic Ocean has been proposed to lead to higher concentrations at Mace Head than observed at remote Scandinavian continental sites (*28*) and a coastal site where the nearby ocean flux is lower than observed at Mace Head (*29*). This trend is however not observed at continental European sites influenced by anthropogenic emissions (*28*).

On August 18th the ship passed 1000 km North of Mace Head and back trajectories indicate that the same northerly air masses received at the ship were transported to Mace Head with a delay of about 2 days (SI S3). Mean GEM at the ship was 1.32 ng/m^3 ($n = 3$) and two days later at Mace Head 1.33 ng/m^3 ($n = 3$) (Hans H. Kock, GKSS, 2010: personal communication). Although this is not an exact comparison it shows good agreement between the independent measurements. Mace Head data thus support the below average summer concentrations found during the NA leg.

During April 21–23 when the ship was 450–850 km from Mace Head, ship and station received air that had been transported at least two days through the MBL, although the origins of the air masses were not identical (SI S3). GEM at the ship was 2.22 ± 0.10 ng/m^3 ($n = 22$) and at Mace Head 1.93 ± 0.04 ng/m^3 ($n = 22$) (Hans H. Kock, GKSS, 2010: personal communication), a difference of 13%. Overall, air arriving at Mace Head spent less time in the MBL than air arriving at the ship. The observed concentrations could be explained if evasion is the main driver of elevated GEM during this season.

A rough estimate of the seasonal variability of GEM above the Atlantic Ocean was made by taking mean concentrations from cruises in the NH Atlantic since 1978 and dividing them by month of measurement, creating a central moving average (Figure 3 and SI T4). It is noted that the measurements arise from campaigns with different methods, duration of sampling, spatial coverage and analytical techniques, and that this analysis overlooks the effect of changes in the source region and meteorology on year to year variation. Nonetheless a seasonal GEM cycle in the Atlantic MBL was found, with minimum concentrations during summer and high concentrations during fall to spring (Figure 3). The seasonal cycle corresponds to the one observed at Mace Head ($r^2 = 0.7$) (*28*) but its amplitude is larger. This suggests a local season-dependent source in the MBL that creates higher concentrations above the ocean surface during some seasons than is seen at coastal sites. This is supported by results from the GEOS-Chem model (*4*).

Influence of Biomass Burning from African Fires. During the first part of the SA leg north of 8°S GEM concentrations were elevated (1.70 ± 0.06 ng/m^3, $n = 13$) and winds came from the southeast (SI S4). Soot data from the ship show elevated concentrations (median absorption coefficient: 1.6(±1.0) × 10^{-6} m^{-1}, $n = 13$) compared to remote ocean sites (0.1 × 10^{-6}–0.5 × 10^{-6} m^{-1}) indicating air masses influenced by biomass burning. This is supported by observations off extensive fires of the Angolan coast (*30*), and by MOPITT (V3) satellite data (*31*) that show high CO column concentrations off the coast in the cruise track between 5°S and 13°S (SI S5, S6). Biomass burning is likely to be the most important source of mercury from Africa (*32*) and previous measurements during African biomass burning episodes have shown an increase over background concentrations of 45% close to the source (*33*). This is in good agreement with the 35% increase that we measured 1000 km from the source. GEM was seen to decrease as the wind direction changed to southerly. Between 13°S and 27°S the ship was no longer intercepting air from the continent and GEM concentrations decreased to SH background levels of 1.3 ng/m^3 ($n = 37$). RGM levels were not increased relative to the rest of the cruise.

African biomass burning is seen to enhance GEM concentrations in the MBL, which most probably leads to enhanced deposition at the ocean surface, although no increase in RGM concentration 1000 km from the coast was observed.

High Levels of GEM and RGM during the Antarctic Summer. The ship intercepted marine air during the AO leg. Close to the Antarctic continent (AC leg) the wind-pattern changed and for two days (24–26 January) the wind came along the coast, which was partly covered with sea ice (*34*), before arriving at the ship (SI S7, S8). From the 26th to 29th of January back trajectories showed a relatively unstable wind direction with air arriving from the coast and the open ocean. These different wind patterns caused a number of changes

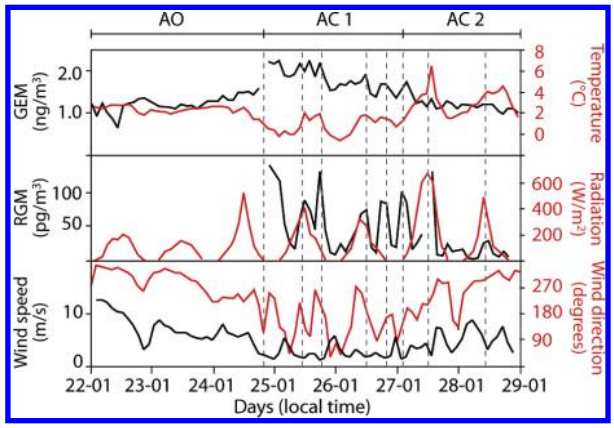

FIGURE 4. Concentrations of GEM, RGM, temperature, radiation, wind speed and wind direction close to the Antarctic continent. Punctuated lines indicate a recurrent pattern of peaks in RGM and GEM observed when wind speed is low, wind direction is from 130−250° and temperature shows small maxima around 2 °C.

in other meteorological parameters and in mercury concentrations (Figure 4).

Maximum insolation increased from 235 W/m^2 for the open ocean to 450−600 W/m^2 close to the continent and wind speed decreased from 15 m/s to a mean of 5 m/s. Temperature decreased from a mean of 2.5 °C in the open ocean to a mean of 0.9 °C between the 24th and the 26th and then increased briefly to 6 °C on the 27th. The change in temperature reflects the origin of the wind: ocean, ice covered surfaces, and finally the ocean again.

On the 24th GEM concentrations increased rapidly from ∼1.3 ng/m^3 to 2.2 ng/m^3 as temperature decreased. GEM remained above the background concentration independent of wind direction until midday on the 27th, when temperature again reached the mean temperature seen prior to the leg (2.5 °C). A decreasing trend in GEM concentrations was observed from the 24th to the 27th over a distance of 150 km. This trend could be explained as dilution with increasing distance from a source.

Eight RGM spikes (30−140 pg/m^3) were observed during the AC leg (Figure 4, punctuated lines). Six of these took place during cold conditions between the 24th and 27th (AC1), and two after (AC2). While no single common factor correlates with all of the general changes seen in the meteorology, a pattern can still be discerned. In the AC leg RGM concentrations always had a midday peak indicating the importance of solar-radiation induced oxidation, but during AC1 4 nighttime peaks were also observed. During AC2 GEM had decreased to background concentrations and the temperature was 2−6 °C. However the oxidation potential still seemed to be large (and wind speed low), giving midday RGM peaks above 30 pg/m^3. This is high relative to typical MBL concentrations, 3 ± 11 pg/m^3.

During AC1 each RGM peak is seen to correlate with a small GEM peak (0.2−0.4 ng/m^3 above baseline for the period) and a temperature between 1.4 and 2 °C, which are small increases relative to a AC1 mean of 0.9 °C. The wind speed decreased to below 3.0 m/s during all RGM peaks, and wind speed and RGM are anticorrelated ($r^2 = 0.3$, $n = 29$). This could be explained by a higher aerodynamic resistance at low wind speeds. A common factor was the wind direction (150−260°) along the coast. Thus it seems likely that the source of GEM during AC1 is areas with partly ice-covered surfaces. GEM could arise by reemission from snow covered surfaces (*35*) or, more likely, evasion due to the release of dissolved gaseous mercury found in a supersaturated environment beneath the ice that is released into the atmosphere as the sea ice breaks up (*10, 36*). Small peaks of GEM during episodes of low wind speed could be caused by an inversion layer. This scenario is consistent with the observation of a downward trend in GEM between the 24th and 27th of January as the ship moves further away from partly ice-covered surfaces.

High concentrations of RGM in the Antarctic austral summer have been observed at Neumayer (*14*) and Terra Nova Bay (*37*). At Neumayer GEM and RGM are anticorrelated (*14*). We know of no previous observations of simultaneous peaks of GEM and RGM during a period of high GEM before. The large fluctuations in RGM concentrations indicate that specific circumstances are needed for high concentrations of RGM to build up. One possibility is that RGM originates from oxidation during transport above sea ice (*14*) or snow. However the four RGM peaks, correlated with maximum radiation, indicate that in these cases oxidation takes place close to the ship, where no sea ice is found (*34*). Relatively large diurnal variability in RGM is also seen after GEM returns to its background level and the wind no longer arrives from along the coast. This indicates that the factors controlling RGM are independent of the GEM source. Volcanic plumes are enriched in bromine (*38*) and fumaroles are located 200 km northeast of the ship at Deception Island (*39*). However the dominant wind direction from southeast and the low wind speed during RGM events makes a scenario with enhanced bromine concentrations from volcanic emissions unlikely. It could be that the normal rate of formation of RGM in the MBL in combination with very low deposition velocity at low wind speed is enough to explain the RGM build up. A normal rate of RGM formation would not affect GEM concentrations, while a low boundary layer height might even slightly enhance concentrations. If this is true high RGM should also be observed in stagnant air arriving at the ship at night (as is the case), as the deposition would be at a minimum.

Acknowledgments

This work was funded by NERI- Aarhus University, The Danish Expedition Foundation, the Villum Kann Rasmussen Foundation, Knud Højgaards Foundation, Andreassens & Hougaards Foundation, Nordea Foundation, the travel fund of the Danish Chemical Society and Carlsbergs Mindelegat. We thank the crew on *Galathea 3*; Bjarne Jensen, Christel Christoffersen, Henrik W. Madsen, Hans Nielsen, Kåre Kemp, and Jørgen Jørgensen for technical support; Matthias Ketzel for soot data; Ralph Ebinghaus and Hans H. Kock for assistance with data from the Mace Head research station; Alexandra Steffen for contribution with equipment; NOAA air resources laboratory (ARL) for the provision of the HYSPLIT transport and dispersion model. This is Galathea3 Contribution No. P65.

Supporting Information Available

Figures S1−S8, Tables Ta1 and Ta2, and four sections of additional text. This material is available free of charge via the Internet at http://pubs.acs.org.

Literature Cited

(1) Mergler, D.; Anderson, H. A.; Chan, L. H. M.; Mahaffey, K. R.; Murray, M.; Sakamoto, M.; Stern, A. H. Methylmercury exposure and health effects in humans: A worldwide concern. *Ambio.* **2007**, *36* (1), 3–11.

(2) Lindberg, S.; Bullock, R.; Ebinghaus, R.; Engstrom, D.; Feng, X. B.; Fitzgerald, W.; Pirrone, N.; Prestbo, E.; Seigneur, C. A synthesis of progress and uncertainties in attributing the sources of mercury in deposition. *Ambio.* **2007**, *36* (1), 19–32.

(3) Strode, S. A.; Jaegle, L.; Selin, N. E.; Jacob, D. J.; Park, R. J.; Yantosca, R. M.; Mason, R. P.; Slemr, F. Air-sea exchange in the global mercury cycle. *Global Biogeochem. Cycles* **2007**, *21* (1), GB1017.

(4) Soerensen, A. L.; Sunderland, E. M.; Skov, H.; Holmes, C.; Jacob, D. J.; Steffen, A. *Modeling Mercury in the Ocean and Its Effect on the Marine Boundary Layer*; ICMPG 2009, Guiyang, China, July 12, 2009; Available at http://acmg.seas.harvard.edu/presentations/.
(5) Mason, R. P.; Rolfhus, K. R.; Fitzgerald, W. F. Mercury in the North Atlantic. *Mar. Chem.* **1998**, *61* (1−2), 37–53.
(6) Temme, C.; Slemr, F.; Ebinghaus, R.; Einax, J. W. Distribution of mercury over the Atlantic Ocean in 1996 and 1999−2001. *Atmos. Environ.* **2003**, *37* (14), 1889–1897.
(7) Lamborg, C. H.; Rolfhus, K. R.; Fitzgerald, W. F.; Kim, G. The atmospheric cycling and air-sea exchange of mercury species in the South and equatorial Atlantic Ocean. *Deep-Sea Res. II* **1999**, *46* (5), 957–977.
(8) Slemr, F. Trends in atmospheric mercury concentrations over the Atlantic Ocean and at the Wank summit, and the resulting constraints on the budget of atmospheric mercury. In *Global and Regional Mercury Cycles: Sources, Fluxes and Mass Balances*; Baeyens, W., Ebinghaus, R., Vasiliev, O. , Eds.; Kluwer Academic Publishers: Netherlands, 1996.
(9) Sommar, J.; Andersson, M. E.; Jacobi, H.-W. Circumpolar measurements of speciated mercury, ozone and carbon monoxide in the boundary layer of the Arctic Ocean. *Atmos. Chem. Phys. Disc.* **2009**, *9*, 20913–20948.
(10) Aspmo, K.; Temme, C.; Berg, T.; Ferrari, C.; Gauchard, P. A.; Fain, X.; Wibetoe, G. Mercury in the atmosphere, snow and melt water ponds in the North Atlantic Ocean during Arctic summer. *Environ. Sci. Technol.* **2006**, *40* (13), 4083–4089.
(11) Laurier, F. J. G.; Mason, R. P.; Whalin, L.; Kato, S. Reactive gaseous mercury formation in the North Pacific Ocean's marine boundary layer: A potential role of halogen chemistry. *J. Geophys. Res., [Atmos.]* **2003**, *108* (D17), 4529.
(12) Laurier, F.; Mason, R. Mercury concentration and speciation in the coastal and open ocean boundary layer. *J. Geophys. Res., [Atmos.]* **2007**, *112* (D6), D06302.
(13) Mason, R. P.; Lawson, N. M.; Sheu, G. R. Mercury in the Atlantic Ocean: Factors controlling air-sea exchange of mercury and its distribution in the upper waters. *Deep-Sea Res. II* **2001**, *48* (13), 2829–2853.
(14) Temme, C.; Einax, J. W.; Ebinghaus, R.; Schroeder, W. H. Measurements of atmospheric mercury species at a coastal site in the Antarctic and over the south Atlantic Ocean during polar summer. *Environ. Sci. Technol.* **2003**, *37* (1), 22–31.
(15) AMAP/UNEP. *Technical Background Report to the Global Atmospheric Mercury Assessment*, Arctic Monitoring and Assessment Programme/UNEP Chemicals Branch, 2008; Available at *www.chem.unep.ch/mercury/*.
(16) Lamborg, C. H.; Fitzgerald, W. F.; O'Donnell, J.; Torgersen, T. A non-steady-state compartmental model of global-scale mercury biogeochemistry with interhemispheric atmospheric gradients. *Geochim. Cosmochim. Acta* **2002**, *66* (7), 1105–1118.
(17) Ariya, P. A.; Skov, H.; Grage, M. M. L.; Goodsite, M. E. Gaseous elemental mercury in the ambient atmosphere: Review of the application of theoretical calculations and experimental studies for determination of reaction coefficients and mechanisms with halogens and other reactants. *Adv. Quantum Chem.* **2008**, *55*, 43–55.
(18) Hedgecock, I. M.; Pirrone, N. Chasing quicksilver: Modeling the atmospheric lifetime of Hg(0)(g) in the marine boundary layer at various latitudes. *Environ. Sci. Technol.* **2004**, *38* (1), 69–76.
(19) Skov, H.; Christensen, J. H.; Goodsite, M. E.; Heidam, N. Z.; Jensen, B.; Wahlin, P.; Geernaert, G. Fate of elemental mercury in the arctic during atmospheric mercury depletion episodes and the load of atmospheric mercury to the arctic. *Environ. Sci. Technol.* **2004**, *38* (8), 2373–2382.
(20) Mason, R. P.; Sheu, G. R. Role of the ocean in the global mercury cycle. *Global Biogeochem. Cycles.* **2002**, *16* (4), 1093.
(21) Holmes, C. D.; Jacob, D. J.; Mason, R. P.; Jaffe, D. A. Sources and deposition of reactive gaseous mercury in the marine atmosphere. *Atmos. Environ.* **2009**, *43* (14), 2278–2285.
(22) Ariya, P. A.; Khalizov, A.; Gidas, A. Reactions of gaseous mercury with atomic and molecular halogens: Kinetics, product studies, and atmospheric implications. *J. Phys. Chem. A* **2002**, *106* (32), 7310–7320.
(23) Goodsite, M. E.; Plane, J. M. C.; Skov, H. A theoretical study of the oxidation of Hg0 to $HgBr_2$ in the troposphere. *Environ. Sci. Technol.* **2004**, *38* (6), 1772–1776.
(24) Vogt, R.; Crutzen, P. J.; Sander, R. A mechanism for halogen release from sea-salt aerosol in the remote marine boundary layer. *Nature.* **1996**, *383* (6598), 327–330.
(25) Witt, M. L. I.; Mather, T. A.; Baker, A. R.; de Hoog, C. J.; Pyle, D. M. Atmospheric trace metals over the south-west Indian Ocean: Total gaseous mercury, aerosol trace metal concentrations and lead isotope ratios. *Mar. Chem.* **2010**, *121* (1−4), 2–16.
(26) Fitzgerald, W. F.; Kim, J. P.; Gill, G. A.; Hewitt, A. D. Atmospheric cycling of mercury over the Pacific Ocean. *Atmos. Environ.* **1986**, *20* (10), 2075–2076.
(27) Draxler, R. P.; Rolph, G. D. *HYSPLIT (HYbrid Single-Particle Lagrangian Integrated Trajectory)*; NOAA Air Resources Laboratory: Silver Spring, MD, 2003; Available at www.arl.noaa.gov/ready/hysplit4.html.
(28) Ebinghaus, R.; Kock, H. H.; Coggins, A. M.; Spain, T. G.; Jennings, S. G.; Temme, C. Long-term measurements of atmospheric mercury at Mace Head, Irish west coast, between 1995 and 2001. *Atmos. Environ.* **2002**, *36* (34), 5267–5276.
(29) Gardfeldt, K.; Sommar, J.; Ferrara, R.; Ceccarini, C.; Lanzillotta, E.; Munthe, J.; Wängberg, I.; Lindqvist, O.; Pirrone, N.; Sprovieri, F.; Pesenti, E.; Strömberg, D. Evasion of mercury from coastal and open waters of the Atlantic Ocean and Mediterranean Sea. *Atmos. Environ.* **2003**, *37* (1), 73–84.
(30) Davies, D. K.; Ilavajhala, S.; Wong, M. M.; Justice, C. O. Fire information for resource management system: Archiving and distributing MODIS active fire data. *IEEE Trans. Geosci. Remote Sens.* **2009**, *47* (9), 3298.
(31) Emmons, L. K.; Edwards, D. P.; Deeter, M. N.; Gille, J. C.; Campos, T.; Nedelec, P.; Novelli, P.; Sachse, G. Measurements of pollution in the troposphere (MOPITT) validation through 2006. *Atmos. Chem. Phys.* **2009**, *9* (5), 1795–1803.
(32) Streets, D. G.; Zhang, Q.; Wu, Y. Projections of global mercury emissions in 2050. *Environ. Sci. Technol.* **2009**, *43* (8), 2983–2988.
(33) Brunke, E. G.; Labuschagne, C.; Slemr, F. Gaseous mercury emissions from a fire in the Cape Peninsula, South Africa, during January 2000. *Geophys. Res. Lett.* **2001**, *28* (8), 1483–1486.
(34) National Ice Center. www.natice.noaa.gov/ (accessed December 2009).
(35) Lindberg, S. E.; Brooks, S.; Lin, C. J.; Scott, K. J.; Landis, M. S.; Stevens, R. K.; Goodsite, M.; Richter, A. Dynamic oxidation of gaseous mercury in the Arctic troposphere at polar sunrise. *Environ. Sci. Technol.* **2002**, *36* (6), 1245–1256.
(36) Andersson, M. E.; Sommar, J.; Gardfeldt, K.; Lindqvist, O. Enhanced concentrations of dissolved gaseous mercury in the surface waters of the Arctic Ocean. *Mar. Chem.* **2008**, *110* (3−4), 190–194.
(37) Sprovieri, F.; Pirrone, N.; Hedgecock, I. M.; Landis, M. S.; Stevens, R. K. Intensive atmospheric mercury measurements at Terra Nova Bay in Antarctica during November and December 2000. *J. Geophys. Res., [Atmos.]* **2002**, *107* (D23), 4722.
(38) von Glasow, R.; Bobrowski, N.; Kern, C. The effects of volcanic eruptions on atmospheric chemistry. *Chem. Geol.* **2009**, *263* (1−4), 131–142.
(39) Global Volcanism Program. www.volcano.si.edu/ (accessed April 2010).

ES903839N